Environ Monit Assess (2009) 152:155–165
DOI 10.1007/s10661-008-0304-8

Characterization and prediction of meandering channel migration in the GIS environment: A case study of the Sabine River in the USA

Joon Heo · Trinh Anh Duc · Hyung-Sik Cho · Sung-Uk Choi

Received: 4 December 2007 / Accepted: 9 April 2008 / Published online: 29 May 2008

Abstract This study focused on the prediction of a 22 km meandering channel migration of the Sabine River between the states of Texas and Louisiana. The meander characteristics of 12 bends, identified from seven orthophotos taken between 1974 and 2004, were acquired in a GIS environment. Based on that earlier years' data acquisition, channel prediction was performed for the two years 1996 and 2004 using least squares estimation and linear extrapolations, yielding a satisfactory agreement with the observations (the median predicted and observed migration rates were 3.1 and 3.6 [m/year], respectively). The best-predicted migration rate was found to be associated with the longest orthophoto-recorded interval. The study confirmed that channel migration is strongly correlated with bend curvature and that the maximum migration rate of the bend corresponded to a radius of curvature [bend radius (R_C)/channel width (W_C)] of 2.5. In tight bends of a smaller radius of curvature than 1.6, secondary flow scouring near the bend apex increases bend curvature. The stability index of the dimensionless bend radius was determined to be 2.45. Overall, this study proves the effectiveness of least squares estimation with historical orthophotography for characterization of meandering channel migration.

Keywords Meandering channel migration · Historical orthophotos · GIS

J. Heo (✉) · T. A. Duc · H.-S. Cho · S.-U. Choi
School of Civil & Environmental Engineering,
Yonsei University, 139 Shinchon-dong,
Seodaemun-gu, Seoul 120-749, Korea
e-mail: jheo@yonsei.ac.kr

Introduction

Meandering rivers have been subject to much and varied analysis owing to their remarkable forms, their ubiquity, their dynamism, and the practical consequences of their movement (Blum et al. 2005; Bridge 2003; Hooke 1995; Kim et al. 1999). Despite decades of research into bank migration prediction, knowledge on the subject is still imperfect, with much work remaining to be done. Accurate mathematical representation of such prediction has yet to be achieved, and the available tools produce results only of varying degrees of uncertainty (Harmar and Clifford 2006; Jang and Shimizu 2005).

Among the available methods, historical photo-interpretation approaches have shown advantages such as time, cost, scale effects, and practical yield (Downward et al. 1995; Aswathy et al. 2007). In fact, historical information sources including maps, air photographs, satellite imagery and cross-sectional surveys have contributed a wealth of information to geomorphological research (Trimble and Cooke 1991), having under-

pinned many studies of river channel change (e.g. Downward 1995; Milton et al. 1995; Kwak and Briaud 2002).

The main obstacles/uncertainties of photo interpretation for meandering channel migration are the resolution of historical photos/maps and the accuracy of methods employed to determine meander characteristics (e.g. bend radius, bend centroid, channel width, bend wavelength). Nowadays, whereas the resolution of images has been dramatically improved to fulfill the interpretation requirement, challenges in optimizing the method of determining meander characteristics remain. Indeed, meander bends are rarely perfectly round with smooth banklines, but often are oddly shaped, with irregular banklines. As a result, identification of the channel centerline or the bend center point can be very difficult. Moreover, the bend radius can differ significantly according to how the bend is bordered, especially with smaller channels. Such identification difficulties can cause random measurement fluctuations for the same margin of bend migration over the time studied.

Based on this fact, least squares estimation for determination of the bend centroid and bend radius of a meander is applied in this study as a solution avoiding or at least limiting the random measurement errors. This approach was used to explore channel change over a small portion of the Sabine River between the American states of Texas and Louisiana, using information derived from aerial photographic coverage for the period between 1974 and 2004, and with refinement of river discharge and regression analyses. The stability of bend morphology is discussed, and the characterization of meanders according to bend radius and wavelength is attempted.

Methodology

There are three methodologies for predicting meander migration: manual overlay techniques, computer-supported techniques, and geographic information system (GIS)-based measurement and extrapolation techniques (Lagasse et al. 2004b). Manual overlay consists of overlaying channel centerlines delineated from successive historic maps or photos that have registered to one another. The inherent problems such as image distortion and scale differences are common problems. This method requires many subjective decisions to determine meander characteristic and it is generally considered as conventional approach. Computer supported technique is the digital version of the manual overlay using typically computer-aided design (CAD) solution and it also suffers from the same problems. On the other hand, GIS-based techniques fully make use of recent digital mapping and database technology. Digital ortho-rectification of historical aerial photography, digital measurement, and spatial analysis in GIS can be applied to measure bend radius, bend centroid, channel width, bend wavelength, etc. Moreover, GIS can load and retrieve these measurements in the database for further analysis. For these reasons, GIS-based techniques for historic assessment and prediction of bend migration were applied in the present study.

Least squares estimation was used to find the center location (centroid) and radius of an imaginary circle best fit to the data points representing the bend line. The equation for this circle with the center—the bend centroid—at (a, b) and radius R is given by:

$$(x-a)^2+(y-b)^2=R^2. \tag{1}$$

Let (x_i, y_i), i=1, 2, …n be a set of data points in the xy plane. To determine the values of a, b, and R that provide a least squares estimation of a circle according to the data points, the following equation was minimized:

$$F(a,b,R)=\sum_{i=1}^{N}\left[(x_i-a)^2+(y_i-b)^2-R^2\right]^2. \tag{2}$$

In addition to the bend radius (R_C) and centroid obtained by least squares estimation, five distance measurements, as part of the bend characterization process, were made. These are the channel widths upstream, at the bend apex and downstream, the bend amplitude, and the bend wavelength. The upstream and downstream channel widths were measured perpendicular to the flow from bankline to bankline at the crossing point between the measured bend and the next upstream or downstream bend. The width of the bend apex was measured perpendicular to the flow from bankline to bankline at the farthest outward extension of the bend. In this study, the channel width value, averaged from the upstream, downstream and apex channel widths, was employed

as the river width/channel width parameter (W_C). The wavelength (W_L) was derived from a line connecting the middle of the channel at the upstream width measurement to the middle of the channel at the downstream width measurement. Then, the wavelength was automatically calculated by doubling the length of this line. Similarly, the bend amplitude (A_m) was calculated by doubling the length of a perpendicular line from the wavelength line to the outer bank of the bend apex where the width was measured. Figure 1 illustrates the geometric parameters of river bend.

Channel migration prediction can be accomplished with two or three historical records per bend, which are used to linearly extrapolate the rates of change in the bend radius and the bend centroid (Lagasse et al. 2004a). For example, if the channel positions and circles inscribed on a bend are recorded in Years 1, 2, and 3 with the corresponding periods of A and B, the bend radius of the predicted year 4 is calculated from the most recent years 3 and 2:

$$R_{C4} = R_{C3} + \left[\left(\frac{(R_{C3} - R_{C2})}{Y_B}\right)(Y_C)\right], \quad (3)$$

where R_{C4} is the Predicted bend radius in Year 4, R_{C3} is the Bend radius in Year 3, R_{C2} is the Bend radius in Year 2, Y_B is the Number of years in Period B, and Y_C is the Number of years in the Period between Year 3 and Year 4. A similar formula is used to predict the magnitude of centroid migration during period C from the most recent period B rate of centroid shift:

$$D_C = \frac{D_B}{Y_B} Y_C, \quad (4)$$

where D_C is the magnitude of centroid migration for Period C, and D_B is the magnitude of centroid migration for Period B. There are two methods of defining the angle of bend migration for Period C. The first is to simply use the same migration angle for Period B (e.g., $\theta_C = \theta_B$). Using the migration angle from the previous period (i.e., Period B) is recommended where geomorphic and hydrologic conditions have not changed significantly or where there are only two historical records available. The second method uses the rate of change of the migration angle from the previous period to define the rate of change for the period being predicted such that

$$\theta_C = \left[\left(\frac{\theta_B - \theta_A}{Y_B}\right)(Y_C)\right] + \theta_B, \quad (5)$$

where θ_C is the Predicted angle of bend migration for Period C, θ_A is the angle of bend migration for Period A, and θ_B is the Angle of bend migration for Period B. The second method can be used where geomorphic, hydrologic, and hydraulic conditions have changed significantly. Based on the natural state of the Sabine River and the time scales of recorded data, the first method was employed in this study

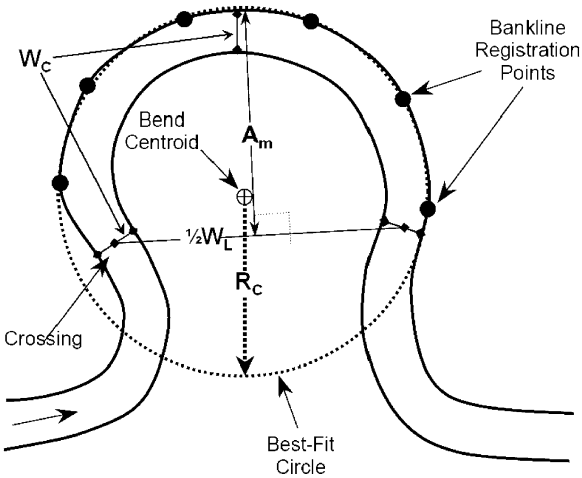

Fig. 1 Illustration of the circle best fitted to a bend

Study area

The studied section of the Sabine River runs north–south from 30°46′36″ N–93°35′06″ W to 30°38′25″ N–93°40′58″W (Fig. 2). This 22 km river section is slow-moving and deep, partially forming the border between the states of Texas and Louisiana. There are numerous sand bars often utilized for camping and other recreational purposes. The river watershed, with a substrate composed of sand, gravel, and mud, takes on a wetland appearance. Vegetation in this area consists largely of water-tolerant hardwoods and grasses. During floods, the terrain usually remains inundated for many days, and sometimes even for several weeks.

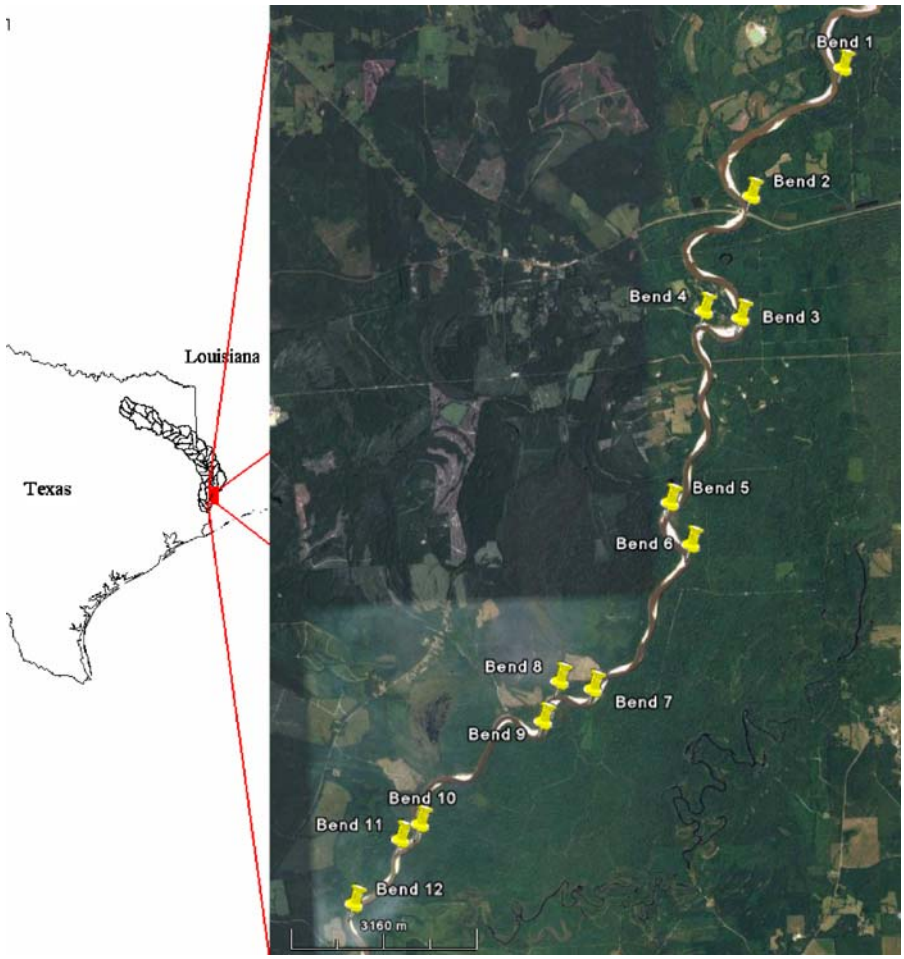

Fig. 2 The Sabine River section and the tested bend locations

The studied area has a coastal climate with mild winters, high annual rainfall, and moderate-to-high humidity. The average annual precipitation is as high as 1,500 mm. Generally, the heaviest rainfall occurs in the late spring, the mid-summer months being the driest. Of the 20 gauges in the basin, the Bon Wier and Ruliff gauging stations are respectively located upstream and downstream of

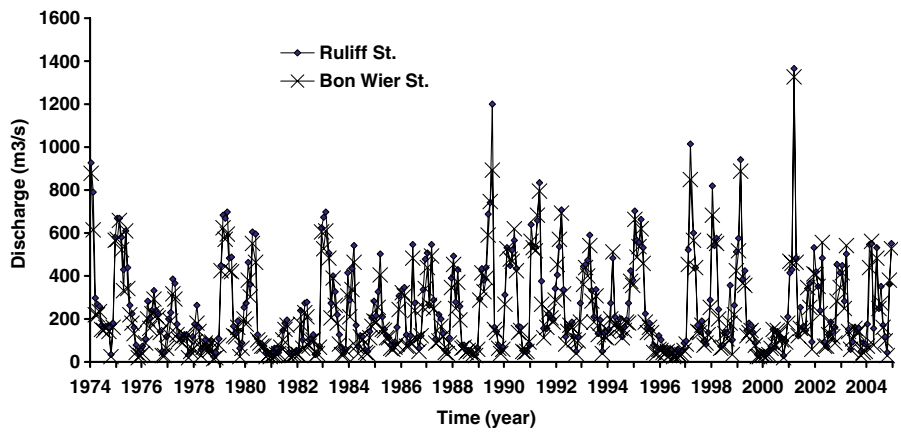

Fig. 3 Monthly discharge at Ruliff (downstream) and Bon Wier (upstream) on the studied river section

Table 1 Average characteristics of the measured bends for different years

Day/ month/ year	Radius	Up. width	Ap. width	Dow. width	Wavelength	Amplitude
29/11/1974	297	183	182	147	1,154	307
27/11/1978	293	159	162	134	1,154	304
04/12/1981	295	161	164	137	1,160	306
15/12/1985	298	163	167	143	1,172	309
16/11/1989	298	163	168	151	1,180	309
12/01/1996	303	161	167	157	1,201	304
12/01/2004	315	162	170	168	1,200	304

the studied section. The historical data from the Bon Wier flow gauge indicate an average annual stream flow of 194 (m^3/s). As shown in Fig. 3, average monthly stream flows generally increase from November to May, then decrease from June to October. This follows the typical rainfall patterns in the basin.

Analysis and discussion

Data acquisition

In the GIS environment, the outer and inner banklines were digitalized from the ortho-rectified images of the 1974, 1978, 1981, 1985, 1989, 1996 and 2004 historical aerial photographs (the precise dates are listed in Table 1). The ortho-rectification used in this study is known as "the second-generation digital orthophoto imagery process", which has become popular throughout the GIS industry as a cost-effective way to replace or update an old digital orthophoto imagery dataset while retaining quick turnaround in production (Merrill 2003). The three process inputs are historical aerial photography, existing DOQQs, and DEMs, which latter are acquired from the USGS. Creating orthophotos requires the following series of processes: (1) interior orientation; (2) block adjustment (exterior orientation); and (3) ortho-rectification. On the whole, the framework of the workflow is the same as that of conventional digital photogrammetry (Fig. 4).

Totally, 12 bends were identified within the studied section, and then the bend radius, center location, wavelength, bend amplitude, and channel width of the 12 identified bends were measured for every considered year. The bend type was classified as the C type, a single-phase meandering channel with point bars and wider bends, according to Thorne (1997). In fact, in this study, the bend radii and centroid positions, correspondingly, were averaged from the outer and inner bend values. The channel width of each bend was calculated as the average of the upstream, apex, and downstream channel widths.

The first interpretation drawn from Table 1 is that, excepting 1974, there is a steady increase of bend radius, channel width, and wavelength over time. The exception for 1974, in which the bend dimensions were relatively larger than in the following years, is attributable to the fact that the 1974 aerial photo was taken during high water (the monthly discharge at the Ruliff gauging station at this time was 580 (m^3/s), the peak discharge of that year). As described in the previous section, the Sabina River in this area is surrounded by wetlands, so high water can temporarily move the banklines landward, leading to falsified bank delineation. Since this high-water effect can render time-comparison channel migration assessment invalid, the 1974 data were not incorporated into the calculations.

Variation of bend characteristics

The variation of bend characteristics along the studied section (Fig. 5) shows that the bend radius and wavelength were sufficiently explanative to characterize the bend morphology and that the channel width and bend amplitude gave little insight into the meander characteristics. For instance, typical visualization of the meanders identifies two very tight bends, no. 4 and 9, which can be determined from the bend radius and wavelength records but which cannot be seen from the channel width and bend amplitude records. The decreasing tendency of channel width and bend amplitude, excepting bend no. 2 where US highway 190 crosses, could be due to other factors such as soil type or vegetation density, which are beyond this study's scope. The work hereafter thus focused on the interpretation of bend radius and wavelength.

A close look at the temporal variation of the bend radius and wavelength indicates that the middle and long bends expanded whereas the tight bends (no. 4 and 9) contracted. The explanation for this opposing variation is the attacking angle and position of the

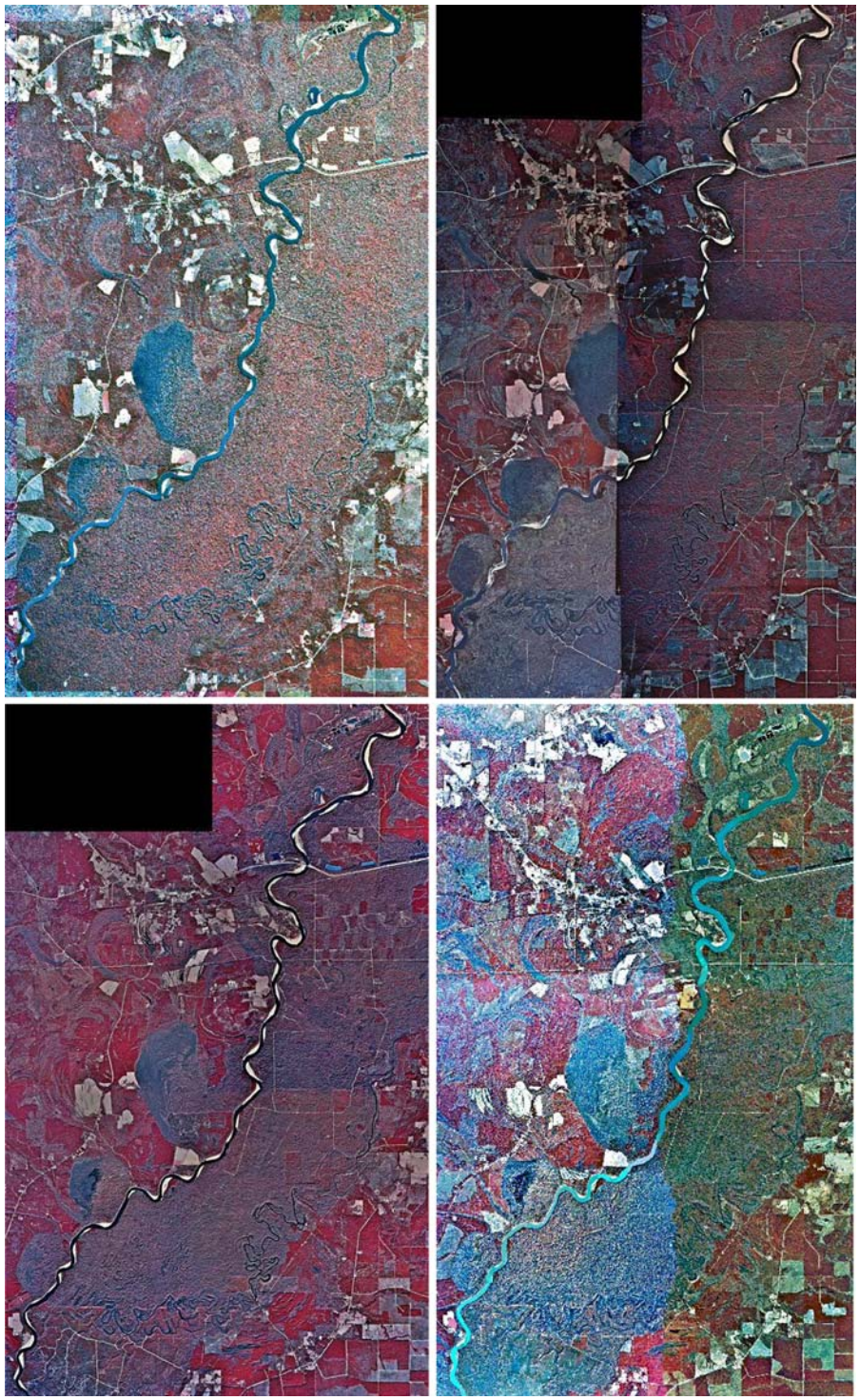

Fig. 4 Presentation of respective orthophotos of 1974, 1989, 1996, and 2004

secondary flow on the outer bank of the meander channel, which has been confirmed as the main cause of bank erosion in various publications (e.g. Ikeda and Parker 1989). Hickin and Nanson (1984) reported that the degree of super elevation of flow and the strength of secondary circulation increase in tighter bends (having a low ratio of bend radius [R_C] to channel width [W_C]). They established that in bends

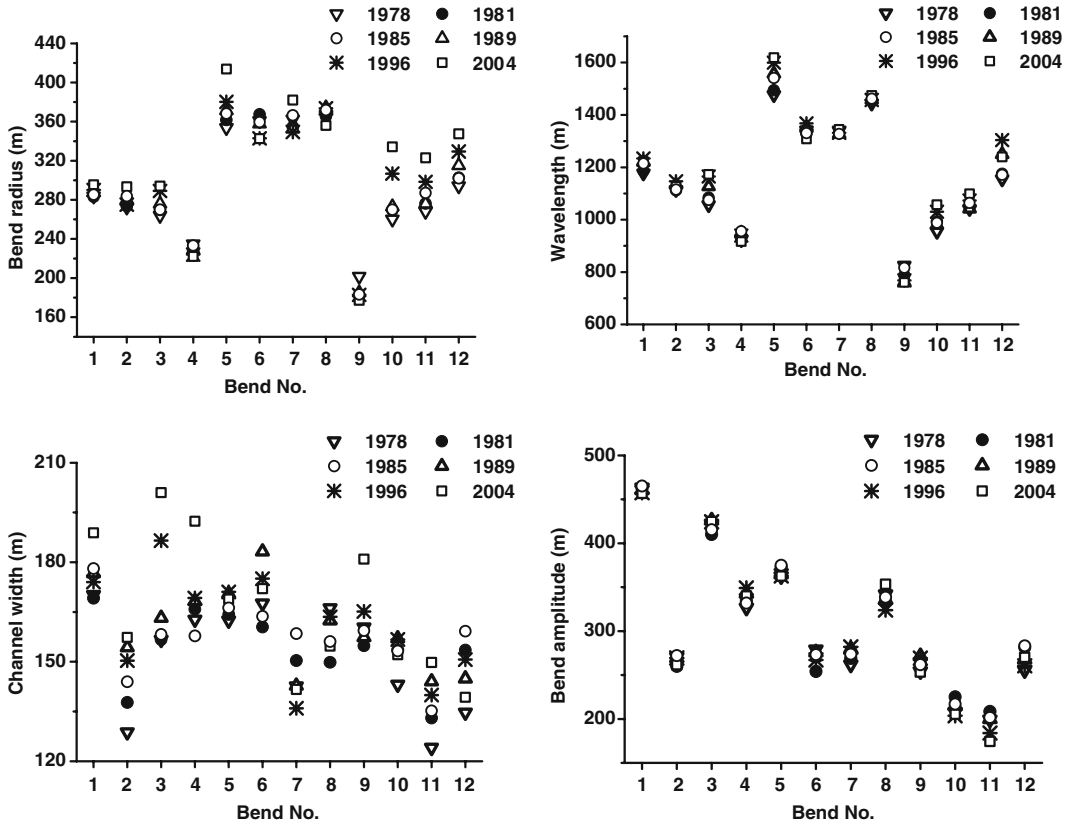

Fig. 5 Representation of bend characteristics for the six considered years

where $R_C/W_C<2$ (the R_C of the outer bank), flow impinges on the outer bank at an acute angle, causing flow separation and generating a strong back eddy along the outer bank near the bend apex. In fact, this acute-angle attack near the apex increases the curvature of the bend (tightens the bend) but might not cause fast migration along the river flow direction. In this case study, for bends Nos. 4 and 9, it was expected that as a bend tightens, the flow approaches the outer bank at a very acute angle, generating extremely severe toe scour, erosion, and bank retreat. As reported by Blanckaert and De Vriend (2004), the point and severity of maximum erosive attack on the outer bank proceeds in stages. For instance, at the intermediate stages, the attack is concentrated between the bend apex and the exit, leading to simultaneous lateral growth and down-valley migration of the bend. However, during high in-bank flows or at a long bend, the point of greatest attack moves downstream of the bend exit, leading to rapid bend migration downstream, which also explains the expansion of long bends in this case study.

Prediction versus observation of bend radius, wavelength, and migration rate (R_T)

The Channel Migration Prediction Tool was used to predict the bend radius, centroid, and orientation angle for 1996 and 2004, based on the bend records of the previous years. Indeed, as the GIS approach is effective

Table 2 Average percentage errors of bend radius, wavelength and migration rate

Period	Predicted	% error radius	% error wavelength	% error migration rate
1978–1989	1996	−1.48	−1.03	−15.42
1981–1989	1996	−1.18	−0.95	−26.04
1978–1989	2004	−3.66	−0.17	−25.59
1981–1989	2004	−2.91	0.06	−24.77
1978–1996	2004	−1.67	1.32	3.21
1981–1996	2004	−1.30	1.49	7.68
1985–1996	2004	−1.47	1.26	15.33
1989–1996	2004	−0.54	2.16	32.05
Average		−1.78	0.52	−4.19

on the decadal scale (emphasized by Gurnell et al. [1998]), the prediction for 1996 and 2004 was based on the bend records of approximately 10-year and longer intervals between 1978 and 1996 (Table 2).

In order to evaluate the applied prediction methods, (1) the bend radius, (2) the magnitude of meander movement and (3) the difference between the predicted and observed meander were focused on. The migration direction of the individual bend was defined as the right angle to the bend orientation angle, which is the angle defined by the line joining the center of the circle to the midpoint of the bend. This angle was measured counterclockwise from a Cartesian-coordinate zero angle defined to be due east.

In general, the predicted results showed good agreement with the observations. The overall average percentage errors were small: −1.78% for the radius, 0.52% for the wavelength, and −4.19% for the migration rate (Table 2). The median predicted and observed migration rates were 3.1 and 3.6 (m/year), within the ranges of 0.65–10.2 and 0.7–10.2 (m/year), respectively. These are moderate rates among free-meander rivers in the USA (Lagasse et al. 2004b). The average predicted radius and wavelength for individual periods were also in good agreement with the observations. That, however, did not describe the migration rate, since six of the averaged eight predicted rates were more than 10% different from the observed ones. Specifically, the poorest prediction results were associated with the shortest time-scale data used for prediction. For instance, the largest underestimation (−26%) was the prediction of the 1996 migration from the 1981–1989 records, and the largest overestimation (32%) was the prediction of the 2004 migration from the 1989–1996 records. By contrast, the best prediction (3.21%) was found to be associated with the longest-interval records (1978–1996). These percentage-error variations again demonstrate that migration prediction based on long-interval/period records is recommended.

For the present case, it can easily be seen that the underestimated migration rates are linked with the migration records prior to 1989. Prior to 1989, as represented in Fig. 3, the intensity and number of bankfull discharges recorded were significantly lower than for later periods, especially the 1989–1996 one. Indeed, river meanders have been widely acknowledged as regulated by flow regime. Therefore, it is rational to posit discharge variation as the principal cause of the migration rate of a meander channel. This, in the present study, was additionally confirmed by the fact that the data recorded in the highest-intensity bankfull discharge period, 1989–1996, lead to an overestimated migration rate for a later year, 2004.

Predicted expansion of bend radius and wavelength: regression analysis

Meander migration is also characterized by radius expansion or contraction. Previous research for various rivers in the USA has shown that tighter bends tend to expand and that longer bends tend to contract by reducing their radius (Spitz et al. 2004). The data set was dominated by a cluster of Radius/Width data points within the 1–3 range and a small change of bend radius (Lagasse et al. 2004b).

Figure 6 shows the ratio of the bend radius for the 3 years 1989, 1996 and 2004 (R_{Cn}) to the bend radius for 1978, the beginning of the studied period (R_{Ci}), plotted versus the bend radius over channel width in 1978 (R_{Ci}/W_{Ci}). An R_{Cn}/R_{Ci} equaling one indicates that the bend did not change its bend radius over the studied period. This data is dominated by data points with $1<R_{Ci}/W_{Ci}<2.6$ and centered on $R_{Cn}/R_{Ci}=1$, similarly to previous research. What was different from the previous research, however, was the fact that the tighter bends (bends no. 4 and 9) tended to contract whereas the others showed some degree of expansion. In Fig. 7, a similar plot is constructed for

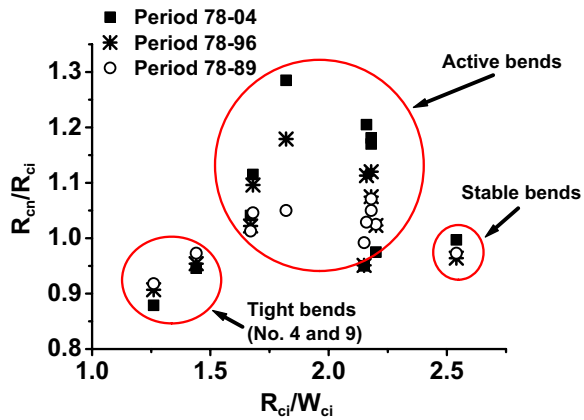

Fig. 6 Change in radius of curvature (R_{Cn}/R_{Ci}) versus radius of curvature/channel width (R_{Ci}/W_{Ci})

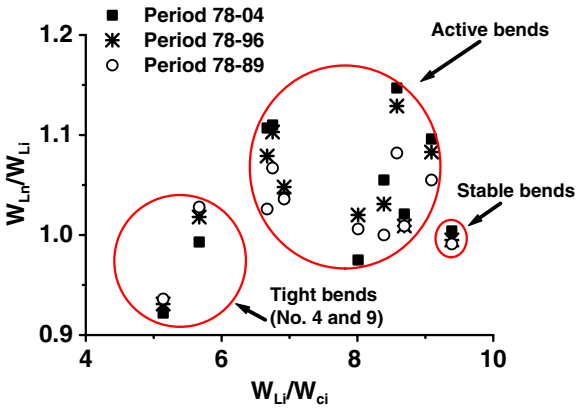

Fig. 7 Change in wavelength (W_{Ln}/W_{Li}) versus initial wavelength/channel width (W_{Li}/W_{Ci})

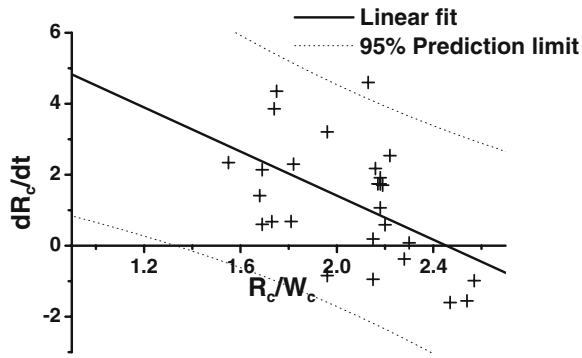

Fig. 8 Linear fit to estimate stable bend radius: $dR_c/dt = -3.11 \times R_C/W_C + 7.63$

the wavelength data, which corresponds to the bend radius change. The wavelengths of tight bends shrunk, of middle bends extended rapidly (active bends), and of long bends did not remarkably extend (stable bends).

Lagasse et al. (2004b) used regression analysis to formulate an empirical equation for calculating the bend radius change over time (t):

$$\frac{dR_C}{dt} = a\left(1 - \frac{R_C}{bW_C}\right)R_C. \quad (6)$$

According to this equation, the coefficient "*b*" is the ratio of bend radius to bend width that is most stable, at least for expansion. However, this does not mean that the bend does not migrate through extension or translation (two other modes of bend migration). When a bend has an R_{Ci}/W_{Ci}="*b*", the bend does not change its radius. For a bend that starts at an $R_{Ci}/W_{Ci} \neq$"*b*", as time progresses, R_{Ci}/W_{Ci} approaches "b" and the rate of change approaches zero. With some refinement, the data on 43 rivers in the USA (Lagasse et al. 2004b) have yielded the equation coefficient "*b*"=2.6. For an R_{Ci}/W_{Ci} less than "*b*", "*a*" is 0.06 and for an R_{Ci}/W_{Ci} greater than "*b*", "*a*" is 0.0025.

Similar to that approach, regression analysis was conducted in the present study to determine the coefficients "*a*" and "*b*" (the data of tight bends No. 4 and 9 were dropped from this analysis, based on the above discussion). In the first step of the analysis, the "*b*" value was determined from a linear fit of the bend radius expansion rate (dR_C/dt) against the radius of curvature (R_C/W_C), as shown in Fig. 8. Then, multivariable fitting of equation 6 was performed to estimate the "*a*" value (Table 3).

The approximated "*b*" value for the bend radius equation was found to be quite similar to the value regressed from the data on the 43 rivers reported in Lagasse et al. (2004b). The value also explains why the studied bends expanded as most of their R_C/W_C indices were smaller than "*b*" (Fig. 8). Thus, all of the bends here should be categorized in the group of tight bends that tend to expand until they reach R_C/W_C="*b*". The "*a*" value for bend radius, the radius expansion rate in physical terms, was found to be smaller than the value regressed from the data on the 43 rivers. This result again proves that the Sabine River exhibits moderate migration.

Bend tightness and migration rate

This study has shown a good correlation between prediction and observation for bend characteristics, especially bend radius, and that correlation is the basis for establishing the relationship between bend tightness, portrayed as bend radius, and migration rate.

Table 3 Regression coefficients to predict expansion of bend radius and wavelength

	b		*a*	
	Value	R^2	Value	R^2
Bend radius	2.45	0.26	0.026	0.38

"a" and "b" are coefficients in equation 6

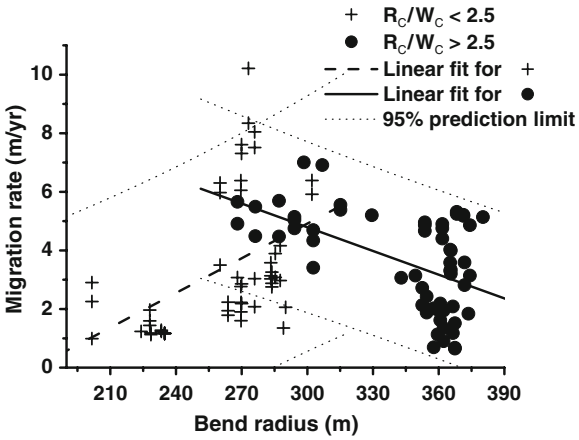

Fig. 9 Regression analysis of migration rate versus bend radius

Indeed, it has long been demonstrated, in fact since Nanson and Hickin (1983) and Harvey (1989), that lateral migration rates of meandering rivers can be correlated with the bend radius of curvature. Normalized migration rates by channel width (R_{TC}) are the highest when the radius of the curvature to channel width ratio (R_C/W_C) is about 2.5, and they are lower when the R_C/W_C is higher and lower owing to the lack of flow convergence and energy loss, respectively. Considerable scatter is apparent in the data, but based on the Beatton River data, Nanson and Hickin (1983) showed that at a R_C/W_C ratio of 2.5, the migration rate, expressed as a ratio of channel widths per year, was maximized (about 0.03 channel widths per year). The present study supports that conclusion, since the highest migration rate was also found to occur at R_C/W_C values of around 2.5.

Similarly to other previous research, too, the bend radii recorded in the present study were distinguished as two groups, the first with the $R_C/W_C<2.5$ and the second with the $R_C/W_C>2.5$ (Fig. 9). Linear regression of these two separate data groups was performed, and the results are shown in Table 4.

As expected, the regression results, in which "b" is negative for bends of $R_C/W_C>2.5$ and positive for bends of $R_C/W_C<2.5$, confirm the maximum bend migration rate of $R_C/W_C=2.5$. Again, the higher R^2 for the bend radius than for the wavelength prove that the bend radius, or in other words the bend tightness, is the proper parameter for meander migration prediction. A comparison with the result reported by Harvey (1989) for the Sacramento River clearly showed that the Sabine River migrated slower than the Sacramento River but faster than 2.5 (m/year), the average rate of the type C meander rivers reported by Thorne (1997).

Conclusions

This study showed the advantage of least squares estimation in determining the bend migration process for a free-meandering channel. The approach implemented in GIS environment, moreover, offered simplicity, robustness, and effectiveness. The technique is especially promising for objective characterization of compound meanders where bends overlap as well as low-sinuosity meanders where bankline curvatures are not fully developed.

Both the predicted and the observed results showed that the Sabine River migrates at a moderate pace among free-meander rivers in the USA. In addition, a comparison between those results indicated that least squares estimation and the GIS-based approach are highly effective for decade-scale images. Also, a temporal analysis showed signs of a bankfull water-discharge-dependant migration rate that is not easily identified by an empirical approach.

Step-by-step analyses of the acquired data proved the importance of the bend radius in migration characterization and prediction. In contrast with the findings from other research in which tight bends reportedly expanded, the very tight bends ($R_C/W_C<1.6$) in the Sabine River contracted as a result of secondary flow scouring near the bend apex. However, regression analysis showed a moderate expanding rate of the river's longer meanders. The regression analysis also indicated the stability index of the dimensionless bend radius to be 2.45, similar to that found by other researchers. There was also clear evidence of the bend-tightness-dependent migration rate in the studied river section, where the maximum migration rate was found at a radius of

Table 4 Linear fit of migration rate versus bend radius

$R_C/W_C<2.5$			$R_C/W_C>2.5$		
a	b	R^2	a	b	R^2
−6.92	0.04	0.20	12.88	−0.03	0.30

"a" and "b" are coefficients in the equation $R_T=a+bR_C$

curvature (R_C/W_C) of 2.5, in agreement with some previous research.

The proposed approach would be beneficial for characterization and prediction of meandering channel migration and, eventually, hydrological planning and management for civil and environmental applications.

References

Aswathy, M. V., Vijith, H., & Satheesh, R. (2007). Factors influencing the sinuosity of Pannagon River, Kottayam, Kerala, India: An assessment using remote sensing and GIS. *Environmental Monitoring and Assessment*, DOI 10.1007/s10661-007-9755-6.

Blanckaert, K., & De Vriend, H. J. (2004). Secondary flow in sharp open-channel bends. *Journal of Fluid Mechanics*, *498*, 353–380.

Blum, M. D., Marriott S. B., & Leclair, S. F. (2005). Fluvial sedimentology, VII. IAS, Blackwell.

Bridge, J. S. (2003). *River and floodplains: Forms, processes and sedimentary records*. Oxford: Blackwell.

Downward, S. R. (1995). Information from topographic survey. In A. M. Gurnell, & G. E. Petts (Eds.), *Changing river channels* (pp. 303–323). Chichester: Wiley.

Downward, S. R., Gurnell, A. M., & Brookes, A. (1995). A Methodology for Quantifying River Channel Planform Change Using GIS Variability. In: J. S. Olive, R. J. Loughrau, J. A. Kesby (Eds.), *Variability in Stream Erosion and Sediment Transport*, IAHS-AISH 224: 449–456.

Gurnell, A. M., Bickerton, M., Angold, P., Bell, D., Morrissey, I., Petts, G. E., et al. (1998). Morphological and ecological change on a meander bend; the role of hydrological processes and the application of GIS. In: A. M. Gurnell, D. Montgomery (Eds.), Hydrological Applications of GIS-1, Hydrological Processes. 12(6), 981–993.

Harmar, O. P., & Clifford, N. J. (2006). Planform dynamics of the Lower Mississippi River. *Earth Surface Processes Landforms*, *31*, 825–843.

Harvey, M. D. (1989). Meanderbelt Dynamics of the Sacramento River. Proceedings, California Riparian Systems Conference, USDA Forest Service General Technical Report PSW-110. 54–61.

Hickin, E. J., & Nanson, G. C. (1984). Lateral migration rates of River Bends. *American Society of Civil Engineers, Journal of Hydraulic Engineering*, *110*, 1557–1567.

Hooke, J. M. (1995). Processes of channel planform change on meandering channels in the UK. In A. Gurnell, & G. Petts (Eds.), *Changes rivers channels* (pp. 87–115). Chichester: Wiley.

Ikeda, S., & Parker, G. (1989). River Meandering. AGU Water Resources Monograph 12.

Jang, C. L., & Shimizu, Y. (2005). Numerical simulation for braided rivers with erodible banks. *KSCE Journal of Civil Engineering*, *9*(5), 429–437.

Kim, J. W., Heo, J. H., & Cho, C. W. (1999). A study on the river bed and hydraulic characteristic changes by flood wave. *KSCE Journal of Civil Engineering*, *3*(3), 243–250.

Kwak, K. S., & Briaud, J. L. (2002). Case study: An analysis of pier scour using the SRICOS method. *KSCE Journal of Civil Engineering*, *6*(3), 243–253.

Lagasse, P. F., Spitz, W. J., Zevenbergen, L. W., & Zachmann, D. W. (2004a). *Handbook for predicting stream meander migration* p. 107. Fort Collins, Colorado: Ayres Associates, Inc.

Lagasse, P., Zevenbergen, L., Spitz, W., & Thorne, C. R. (2004b). *Methodology for predicting channel migration* p. 214. Fort Collins, Colorado: Ayres Associates, Inc.

Merrill, P. B. (2003). Second Generation Orthophotography: Why? *Proceedings of the Twenty Third Annual ESRI User Conference*, Redland, CA, USA.

Milton, E. J., Gilvear, D. J., & Hooper, I. (1995). Investigating change in fluvial systems using remotely-sensed data. In A. M. Gurnell, & G. E. Petts (Eds.), *Changing river channels* (pp. 277–301). Chichester: Wiley.

Nanson, G. C., & Hickin, E. J. (1983). Channel migration and incision on the Beatton River. *Journal of Hydraulic Engineering*, ASCE, 109.

Spitz, W., Lagasse, P. Schumm, S., & Zevenbergen, L. (2004). A methodology for predicting channel migration. NCHRP Project No. 24-16.

Thorne, C. R. (1997). Channel types and morphological classification. In C. R. Thorne, R. D. Hey, & M. D. Newsom (Eds.), *Applied fluvial geomorphology for river engineering and management*. Chichester, UK: John Wiley and Sons.

Trimble, S. W., & Cooke, R. U. (1991). Historical sources for geomorphological research in the United States. *Professional Geographer*, *43*, 212–228.